Residual Dopant Levels in Silicon Feedstock Grown by Pilot-Scale Atmospheric Pressure Iodine Vapor Transport

T.F. Ciszek

Siliconsultant Division of Geolite, Evergreen, Colorado, 80439, USA

Abstract — **The atmospheric pressure iodine vapor transport method for polysilicon feedstock generation from metallurgical-grade silicon was introduced in 2002. More recent industrial pilot-scale development of the process has produced feedstock with improved electrically-active impurity control. Czochralski single crystal growth was carried out using relatively recent polysilicon produced by this method. The polysilicon was found to produce n-type single crystal material with some compensating p-type component. The resistivity data could be approximately fit to normal freezing curves with initial P and B concentrations of $C_o = 1.1 \times 10^{15}$ and $C_o = 3.3 \times 10^{14}$ atoms·cm^{-3} respectively.**

Index Terms — **silicon, feedstock, crystal growth, dopant levels**

I. BACKGROUND AND INTRODUCTION

In 2002, Wang and Ciszek introduced an atmospheric-pressure iodine vapor transport (APIVT) method for producing polysilicon feedstock directly from metallurgical grade (MG) silicon [1]. This arose from earlier work on growth of thin epitaxial silicon layers by APIVT [2], [3]. The approach was further refined in 2004 [4]. Preliminary results on silicon feedstock production by APIVT were presented in 2002 [5]. Industrial pilot-level scale-up of the process has since been carried out. Results of Czochralski (CZ) growth and residual dopant levels in this more-recent material are presented here.

The basic principle of the APIVT process is shown in Fig. 1. APIVT of silicon takes place via a disproportionation reaction between components SiI_2 and SiI_4. It is a high-temperature T_h to low temperature T_c deposition process taking place at atmospheric pressure. Iodine reacts with the source MG silicon in the higher temperature region to form SiI_4 which further reacts with silicon to make SiI_2. The SiI_2 transports from T_h to T_c where Si is deposited on the substrate and the resulting SiI_4 migrates to T_h where it then picks up more Si maintaining the cycle. It is a non-vacuum, open-chamber, cold-wall deposition technique. More details are available in [6].

Iodine vapor transport purification shows promise for reducing the concentration of most MG-Si impurities more than several orders of magnitude to near-acceptable levels for PV feedstock [5]. The purification occurs by two mechanisms: (1) During the initial reaction between I and MG-Si, formation of impurity iodides will be advanced or retarded depending on their free energies of formation and (2) Some metal iodides are more stable than SiI_2 and SiI_4, forming readily in the gas phase, but having only a small tendency for reduction in the deposition zone. However, further impurity reduction would be beneficial and is essential for B, C, and P. References [1] and [4] address this by incorporating an in situ distillation step schematically shown in Fig. 2 to remove impurity-iodide byproducts.
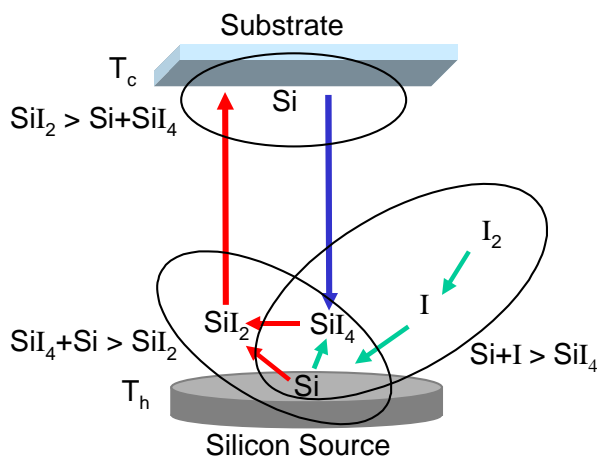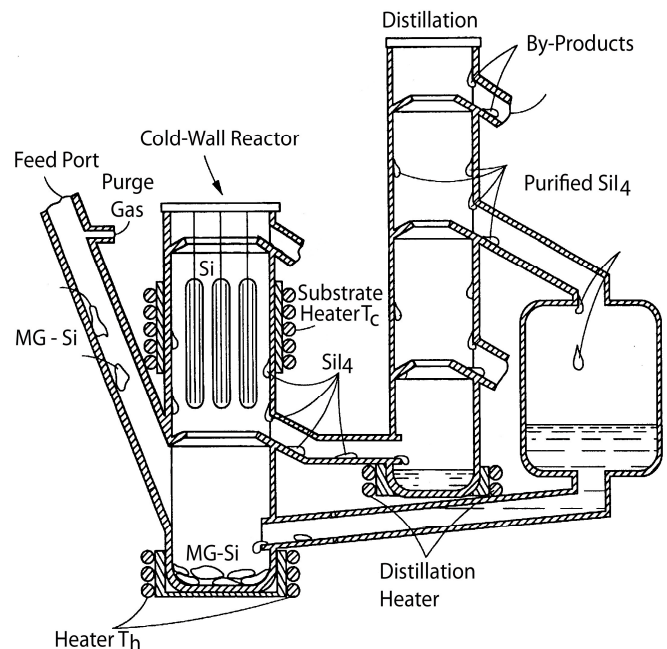

Fig. 1. The APIVT process (from [6])

Fig. 2. APIVT incorporating distillation purification (from [4]).

II. Experimental

We investigated two polysilicon samples produced in the 2012 time-frame by a private company working on pilot-level scale-up of the APIVT process. The polysilicon was grown on a Si rod substrate with square cross-section. We sawed slabs of the polysilicon away from the substrate to isolate the grown poly from the substrate, cleaned and acid-etched them, and loaded the 48 g charge into a quartz crucible (Fig. 3) for lab-scale CZ crystal growth.

Fig. 3. APIVT polysilicon slabs in a quartz crucible for CZ growth

The deposited material from the early part of the time-frame had significant porosity as shown in the cross-section (Fig. 4). Also, yellowish-white deposits of a foreign material were noticed particularly at the four corner-edges of the deposited material. These were ground away for the most part prior to etching. Upon melting the charge, significant oxides were seen
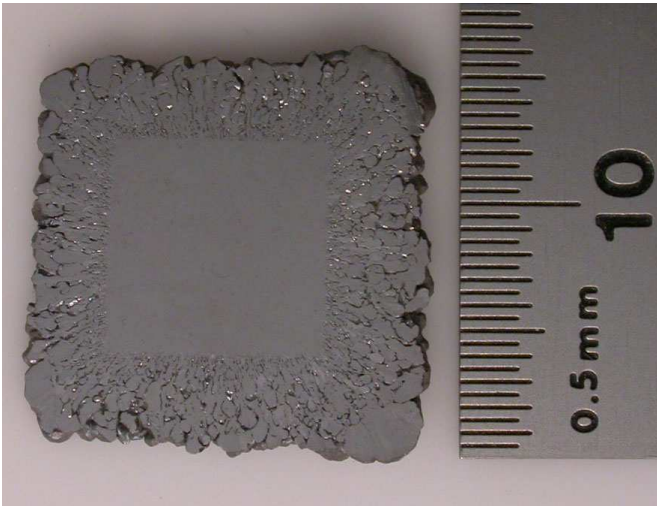

Fig. 4. Cross-section of porous APIVT deposit on an 8mm x8mm square cross-section single crystal rod substrate.

to evolve from the melt and solid clusters formed on the crucible wall above the melt. However, [100] single crystal growth could be initiated although it later twinned with one (111) twin plane, but otherwise remained single. The resultant 22mm diameter crystal had an oxide surface coating (Fig. 5). Crystal growth was carried out in an argon ambient at 3 liter·min^{-1} flow rate using 2mm·min^{-1} pull speed, a 19 rpm crystal rotation rate, and a 15 rpm crucible rotation rate.

Fig. 5. Twinned [100] crystal

The entire crystal was N-type. The average of 5 thick-sample, 4-probe resistivity measurements made at a g value (fraction solidified) of 0.16 was 2.56 Ω-cm with a standard deviation of $\pm$ 0.03. At g = 0.43 it was 1.89 Ω-cm $\pm$ 0.02. The graph in Fig. 6 places the concentrations corresponding to the resistivity results (▲) on the normal freezing curve

$$C = k_{eff}C_o(1\text{-}g)^{k_{eff}-1} \qquad (1)$$

for k_{eff} = 0.35 and C_o = 4.89 x 10^{15} atoms·cm^{-3}, which makes a reasonably strong case for the major dopant being phosphorous at a concentration near 4.9 x 10^{15} atoms·cm^{-3}, since the k_{eff} for phosphorous is 0.35 and the crystal is N-type.
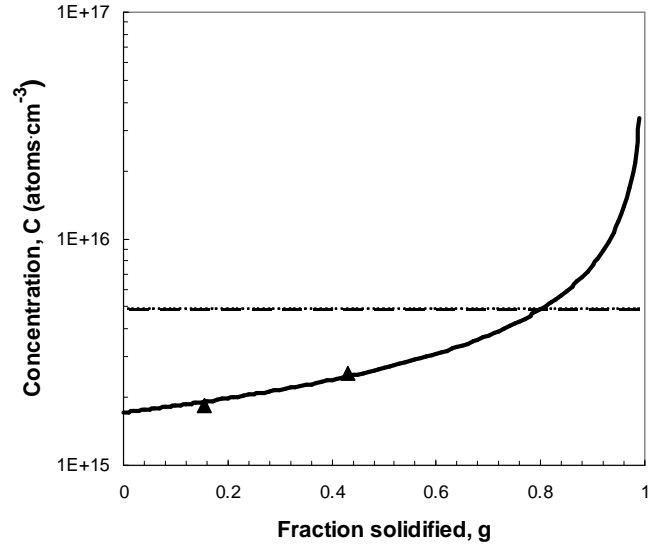

Fig. 6. Impurity concentrations corresponding to observed resistivity measurements on a normal freezing curve for k_{eff} = 0.35 and C_o = 4.89 x 10^{15} atoms·cm^{-3}

However, because the data point at g = 0.16 lies slightly below the normal freezing curve, and the one at g = 0.43 slightly above, there is probably a small amount of p-type compensation.

The 2nd sample was produced later in the 2012 time-frame. Its cross-section is shown in Fig. 7. The substrate for both this and the deposit shown in Fig. 4 was an 8mm x 8mm cross-section single crystal silicon rod. The 2nd sample had more growth on the substrate and the deposit was less porous. The dark smudges in the lower region are residual saw slurry and not inherent to the sample. A similar CZ growth procedure was followed as for the 1st sample. The melt was much freer of oxide evolution and it was possible to initiate [100] dislocation-free crystal growth (Fig. 8). The crystal was completely single-crystalline. It and the Si left in the crucible were clean and shiny (Fig. 9). Five resistivity measurements were made at each of four locations and the average values are presented in Table I, along with the value of the corresponding
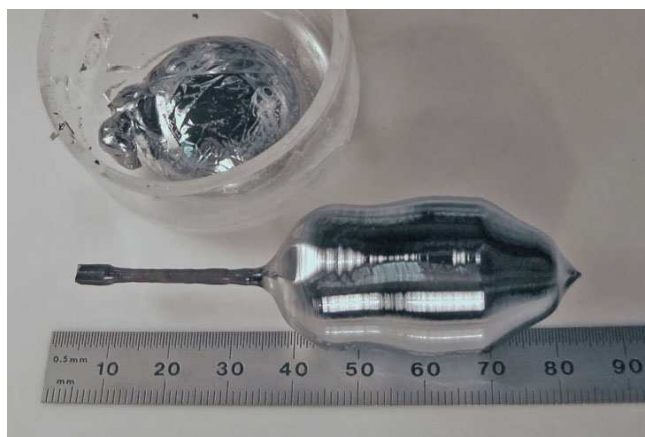

Fig. 9.   [100] dislocation-free crystal and melt residue after growth

TABLE I
AVERAGE RESISTIVITY MEASURED AT FOUR VALUES OF g
FRACTION SOLIDIFIED

Fraction Solidified, g	Resistivity ρ, Ω-cm	Conductivity Type
.10	34 ± 2	N
.23	22 ± 2	N
.56	13 ± 1	N
.68	$10.1 \pm .5$	N

fraction solidified, g. This crystal was also N-type and it had a higher resistivity. The graph in Fig. 10 places the N-type concentrations (black triangles) corresponding to the four average resistivities on a plot of C vs. g, assuming only an N-type dopant with no compensation from P-type dopants. A best-fit normal freezing curve is also fitted to the 4 data points, for $k_{eff} = 0.35$. The best-fit value for C_o is 5.45×10^{14} atoms·cm^{-3}, assuming phosphorous is the only dopant.

Fig. 7.   Cross-section of 2nd APIVT polysilicon sample

Fig. 8.   [100] dislocation-free growth with 2nd APIVT Si sample

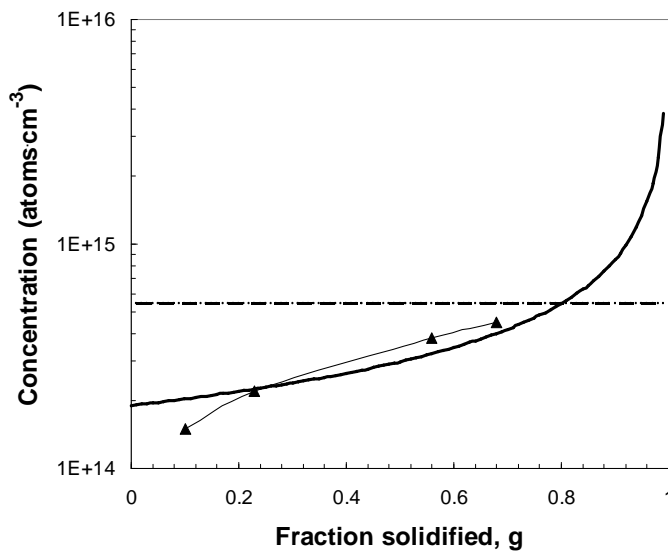Fig. 10.   Impurity concentrations corresponding to observed resistivity measurements on a normal freezing curve for $k_{eff} = 0.35$ and $C_o = 5.45 \times 10^{14}$ atoms·cm^{-3}

As can be seen from the trend line of the data points, the fit is not very good and there is evidence of a compensating P-type component. A better correlation with the observed resistivity values is obtained with two normal freezing curves, one for phosphorus with $k_{eff} = 0.35$ and $C_o = 1.13 \times 10^{15}$ atoms$\cdot$cm^{-3}; the other for boron with $k_{eff} = 0.80$ and $C_o = 3.3 \times 10^{14}$ atoms$\cdot$cm^{-3}. Fig. 11 shows the normal freezing curves for phosphorous (green) and boron (black) and their corresponding C_o's (horizontal lines). The N-type resistivities corresponding to the differences between the phosphorous concentrations (▲) and the boron concentrations (▲) at the four values of g are compared in Table II with the measured resistivities at those g values.
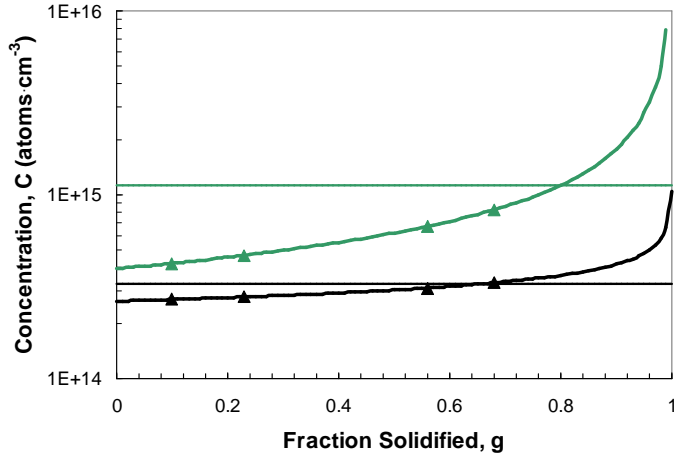

Fig. 11. Calculated normal freezing curves and C_o's (horizontal lines) for phosphorous (shown in green) and boron (in black) for which the differences in concentration C give a best fit to the measured resistivities.

TABLE II

COMPARISON OF MEASURED RESISTIVITIES WITH CALCULATED VALUES FROM FIG. 11, FOR $C_o = 1.13 \times 10^{15}$ ATOMS$\cdot$CM^{-3} FOR PHOSPHOROUS AND $C_o = 3.3 \times 10^{14}$ ATOMS$\cdot$CM^{-3} FOR BORON

Fraction Solidified, g	Resistivity ρ, Ω-cm (measured)	Resistivity ρ, Ω-cm (calculated, Fig. 11)
.10	34	32.8
.23	22	26.0
.56	13	13.6
.68	10.1	10.0

III. DISCUSSION AND CONCLUSIONS

Polysilicon samples from pilot-scale deposition by the atmospheric-pressure iodine vapor transport APIVT technique were tested for utility as a feedstock for CZ crystal growth using lab-scale growth apparatus. Polysilicon grown in early 2012 had high oxide content and high porosity. The CZ crystal grown from it was prone to twining. It was N-type with resistivity in the 1 – 3 Ω-cm range, and the predominant residual electrically-active dopant appears to be phosphorous at concentration $C_o \cong 4.9 \times 10^{15}$ atoms$\cdot$cm^{-3}. A second sample, grown later, had much less porosity and a dislocation-free [100] crystal could be grown with minimal oxide deposit. It was also N-type and had a higher resistivity, in the 10-40 Ω-cm range. It appears to have compensating residual electrically active dopants, and normal freezing curves (1) calculated for phosphorous at $C_o \cong 1.13 \times 10^{15}$ atoms$\cdot$cm^{-3} and boron at $C_o \cong 3.3 \times 10^{14}$ atoms$\cdot$cm^{-3} were fitted to the observed 4-probe resistivity measurements.

REFERENCES

[1] Tihu Wang and Theodore F. Ciszek, "Purification and Deposition of Silicon by an Iodide Disproportionation Reaction," U.S. Patent 6,468,886 (2002).
[2] T.H. Wang, T.F. Ciszek, M. Page, Y. Yan, R. Bauer, Q. Wang, J. Casey, R. Reedy, R. Matson, R. Ahrenkiel, and M. M. Al-Jassim, "Material Properties of Poly-Silicon Layers deposited by Atmospheric Pressure Iodine Vapor Transport," Conf. Record of the 28th IEEE PVSC, September 2000, Anchorage, p.138-141.
[3] T.H. Wang, T.F. Ciszek, M.R. Page, R.E. Bauer, Q. Wang, and M.D. Landry, "APIVT-Grown Silicon Thin Layers and PV Devices," in: 29th IEEE Photovoltaic Specialist Conf. Record, New Orleans, LA, May 2002 (IEEE, New Jersey, 2002) pp. 94-97.
[4] Tihu Wang and Theodore F. Ciszek, "Purified Silicon Production System," U.S. Patent 6,712,908 B2 (Mar. 30, 2004).
[5] T.F. Ciszek, T.H. Wang, M.R. Page, R.E. Bauer, and M.D. Landry, "Solar-Grade Silicon from Metallurgical-Grade Silicon via Iodine Chemical Vapor Transport Purification," in: 29th IEEE Photovoltaic Specialist Conf. Record, New Orleans, LA, May 2002 (IEEE, New Jersey, 2002) pp. 206-209.
[6] T.H. Wang, T.F. Ciszek, M.R. Page, R.E. Bauer, and M.D. Landry, "Thin Layer Si Growth by Atmospheric Pressure Iodine Vapor Transport," 11th Workshop on Crystalline Silicon Solar Cell Materials & Processes, August 19-22, 2001, Estes Park, CO, NREL/BK-520-30838, pp. 155-158.